

PACS numbers: 42.60.Da; 42.60.Jf; 42.55.Rz
DOI: 10.1070/QE2007v037n02ABEH013430

Generation of high-order Hermite – Gaussian modes in a flashlamp-pumped neodymium phosphate glass laser and their conversion to Laguerre – Gaussian modes

A.A. Malyutin, V.A. Ilyukhin

***Abstract*.** **The Hermite – Gaussian modes up to the third order inclusive are generated in a flashlamp-pumped neodymium phosphate laser and converted to the corresponding Laguerre – Gaussian modes in an astigmatic $\pi/2$ converter. It is also shown that, by using a laser with the gain minimum on the axis of a plane – spherical resonator and changing its Fresnel number, it is possible to excite efficiently Laguerre – Gaussian modes with the field amplitude dependence $\sim {\sin \atop \cos}(l\varphi)$.**

Keywords: *pulsed Nd^{3+} : glass laser, inverse population distribution, Hermite – Gaussian modes, Laguerre – Gaussian modes, astigmatic $\pi/2$ mode converter.*

1. Introduction

The generation of high-order Hermite – Gaussian or Laguerre – Gaussian modes in pulsed solid-state lasers was a quite common effect at the dawn of the development of quantum electronics. The main goal at first was to achieve the maximum output radiation energy and power by using resonators with large Fresnel numbers. Later, it became clear that laser radiation with strictly specified properties should be used in experiments and practical applications. This required the knowledge of the basic parameters of a laser beam such the wavelength, energy, pulse duration and shape, and near- and far-field radiation intensity distributions. The standardisation of methods for measuring all these parameters, needed for a comparison of the results of independent studies, is being continued at present [1]. As a rule, researchers (followed by laser companies) prefer laser beams with the intensity distribution close to the lowest Hermite – Gaussian (HG) TEM_{00} mode with the generalised spatial-angular parameter M^2 close to unity. The properties of such radiation propagating to any spatial point (when optics that does not break paraxiality is used) can be easily calculated. The best results on excitation of the TEM_{00} mode in lasers of different types are achieved by using Gaussian apertures or mirrors with the Gaussian distribution of the reflection coefficient in unstable resonators (see review [2]).

There exist, however, situations when higher-order HG modes are required. An example is the use of the $u_{mn}^{\rm HG}$ modes to obtain with the help of $\pi/2$ converters [3 – 5] the Laguerre – Gaussian (LG) $u_{pl}^{\rm LG}$ modes [$p = \min(m, n)$, $l = m - n$] having the nonzero orbital angular momentum, the circular intensity distribution, and a singularity (nonzero values of the amplitude and phase) on the beam axis. Such beams are recently used for investigations in atomic physics, microhydrodynamics, biology, and nanotechnology [6 – 9].

The ratio of the radius of a beam of the mode of the order $N = m + n = 2p + l$ to that of the mode with $N = 0$ in stable resonators is $(N + 1)^{1/2}$. Therefore, if the fundamental mode can be excited by suppressing all the other modes in a resonator at a Fresnel number $N_{\rm F} = a^2/\lambda L$ (a and L are the aperture radius and resonator length, respectively), then to excite the mode of the order N, by providing the same loss level, the Fresnel number of the resonator should be increased up to $\sim N_{\rm F}(N + 1)$. However in this case, a laser will emit, as a rule, many modes of orders in the range from 0 to N. Their number and the ratio of intensities are functions of the pump level, resonator parameters, the position of an active medium in the resonator, and frequency selecting elements. The type of inversion distribution in the active element also plays an important role. The latter factor together with the choice of the resonator geometry to form a particular type of oscillations can be most simply used upon diode pumping of active media (see references in [10]). The selection of transverse modes in usual lasers has long been performed by using thin intracavity wires, which give good results at least for a He – Ne laser.

The aim of this paper was to generate pure higher-order HG modes in a flashlamp-pumped neodymium phosphate glass laser. This was achieved by using above-mentioned spatial selectors (thin wires) located on the resonator axis. The quality of generated HG modes was verified by transforming them to the LG modes with the help of an astigmatic $\pi/2$ converter, which is a rather sensitive tool for determining the amplitude and, especially, phase distortions of initial laser beams. We also made an attempt to determine the influence of the inverse population (IP) distribution in the active medium on the purity of excited types of oscillations.

2. Experimental

We used in experiments a plane – spherical resonator of length $L = 50$ cm with the radius of curvature of a highly

A.A. Malyutin A.M. Prokhorov General Physics Institute, Russian Academy of Sciences, ul. Vavilova 38, 119991 Moscow, Russia; e-mail: amal@kapella.gpi.ru;
V.A. Ilyukhin Moscow Engineering and Physics Institute (State University), Kashirskoe sh. 31, 115409 Moscow, Russia

Received 18 September 2006
Kvantovaya Elektronika **37** (2) 181 – 186 (2007)
Translated by M.N. Sapozhnikov

reflecting mirror $R = 300$ cm. A selector of longitudinal modes [11] with the maximum of the reflection coefficient $\sim 45\,\%$ was used as the output plane mirror. The active elements (AEs) of the laser were made of a GLS-23 neodymium phosphate glass, they had plane–parallel ends tilted at an angle of 85° to the resonator axis and were 5×100 or 7×130 mm in size (depending on the pump cavity type). An AE of diameter 7 mm was placed either into a one-lamp pump cavity with a quartz elliptical mirror reflector or into the cavity with a diffusion reflector providing the dense AE–flashlamp packing (both reflectors had a length of 90 mm). An AE of diameter 5 mm was mounted only inside a one-lamp pump cavity with a quartz elliptical mirror reflector of length 60 mm. We used in experiments, unless otherwise stated, passive Q-switching with the help of a $F_2^- : LiF$ Q switch.

2.1 Measurement of the inverse population profile

The optical scheme for measuring the IP profile is shown in Fig. 1. The AE end was imaged with a reduction of 0.7 by a lens with the focal distance 50 cm on a CCD array detector of an ELPHEL 313 camera [12]. A 2-mm aperture restricted the collection of radiation from the AE volume by the solid angle $\Omega \approx 2.5 \times 10^{-5}$ rad.

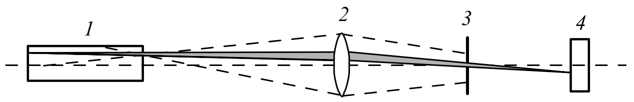

Figure 1. Scheme of the measurement of the inverse-population distribution in a GLS-23P glass active element of a laser; (*1*) AE; (*2*) lens; (*3*) aperture; (*4*) diode array detector.

By assuming that the IP in the AE slowly varies in time and has the same distribution $n(x, y, t)$ in all sections $0 \leqslant z \leqslant L_a$ (L_a is the AE length) of the active medium, we obtain the energy

$$dE \sim \gamma n(x, y, t)\Omega dz dt \quad (1)$$

emitted into the solid angle Ω by the volume element of the active medium of thickness dz for the time dt satisfying the condition $\tau \ll dt \ll T$, where $\tau = L_a/c$ and T is the spontaneous radiation pulse duration (γ is the proportionality coefficient). In the case of unsaturated amplification, the radiation energy at the AE output emitted for the time dt is

$$E(x, y, t) \sim \gamma n(x, y, t)\Omega dt \int_0^{L_a} \exp[\sigma n(x, y, t)(L_a - z)dt]dz$$

$$= \frac{\gamma\Omega \exp[\sigma n(x, y, t)L_a dt] - 1}{\sigma}, \quad (2)$$

where σ is the stimulated emission cross section. It is obvious that $n(x, y, t)$ can be represented in the form

$$n(x, y, t) = n_{\max}(x, y)f(t), \quad (3)$$

where $f(t)$ is the IP variation in time and $n_{\max}(x, y)$ is the maximum IP value at the point (x, y). Then, the energy

$$E_0(x, y) \sim \frac{\gamma\Omega \exp\left[\sigma n_{\max}(x, y)L_a \int_0^T f(t)dt\right] - 1}{\sigma}$$

$$= \frac{\gamma\Omega \exp[\sigma n_{\max}(x, y)f_0 L_a] - 1}{\sigma} \quad (4)$$

is emitted within the solid angle Ω during the pulse, where $f_0 = \int_0^T f(t)dt$ is the form factor of the spontaneous radiation pulse. For moderate gains in the AE, expression (4) is reduced to the form

$$E_0(x, y) \sim \gamma\Omega f_0 L_a n_{\max}(x, y), \quad (5)$$

so that the energy $E_0(x, y)$ recorded with a photodetector describes the IP distribution over the AE section. The results of the measurements are presented in Fig. 2. Figure 2d shows the IP distributions in the flashlamp–AE plane normalised to the maximum value. All the measurements were performed by using simmer discharge and 50 J of stored energy in the pumping system, which was equivalent to the gain per transit in the AE of no more than 1.5.

As follows from Fig. 2, when the AE of diameter 7 mm was used in the laser with the elliptic mirror reflector, the maximum of the gain distribution almost exactly coincided with the AE axis. This distribution (within the IP values 0.6–1) can be approximated by a Gaussian with the characteristic radius $w_g \approx 1.3$ mm.

The region with the maximum IP value in the diffusion reflector is adjacent to the flashlamp. And although it seems that the IP is homogeneously distributed over a large area of the AE, the presence of the inversion minimum (at a distance of ~ 1 mm from the AE axis) affects, as will be shown below, the type of lasing.

The visual difference between IP distributions for mirror reflectors in Fig. 2a (AE of diameter 7 mm) and Fig. 2c (AE of diameter 5 mm) is small. However, the IP in the latter case varies as a whole more uniformly: the approximation of the corresponding curve in Fig. 2d by a Gaussian gives the characteristic radius $w_g \approx 3.6$ mm.

2.2 Lasing parameters

Consider first the emission parameters of lasers with the above-mentioned IP distributions in the AE which were obtained for the case of Fig. 2b (diffusion reflector). This distribution proved to be unsuitable for generating HG modes. The main reason is the increase in the gain from the centre of the region with the 'homogeneous' IP distribution to its edge. Such a variation in the gain can be considered as the use of an intracavity 'aperture with an inverse Gaussian distribution' [13] producing a strong mode instability. Theoretically in this case, small perturbations of the radiation field amplified in an AE of an unlimited cross section lead to an infinite increase in the field at the laser beam periphery [14]. In practice, due to the finite AE aperture this results in the generation of the LG modes, whose order increases with increasing the Fresnel number of the resonator. Thus, when the axis of a plane–spherical resonator is displaced to the homogeneous IP region (to suppress lasing in the AE region adjacent to the flashlamp, see Fig. 2b) and any aperture limitations except the AE (with the effective diameter 6 mm) are absent, the laser emits at the LG mode with $N \approx 18$ [the dependence of the amplitude on the polar angle is $\sim {\sin \atop \cos}(l\varphi)$, Fig. 3a]. When

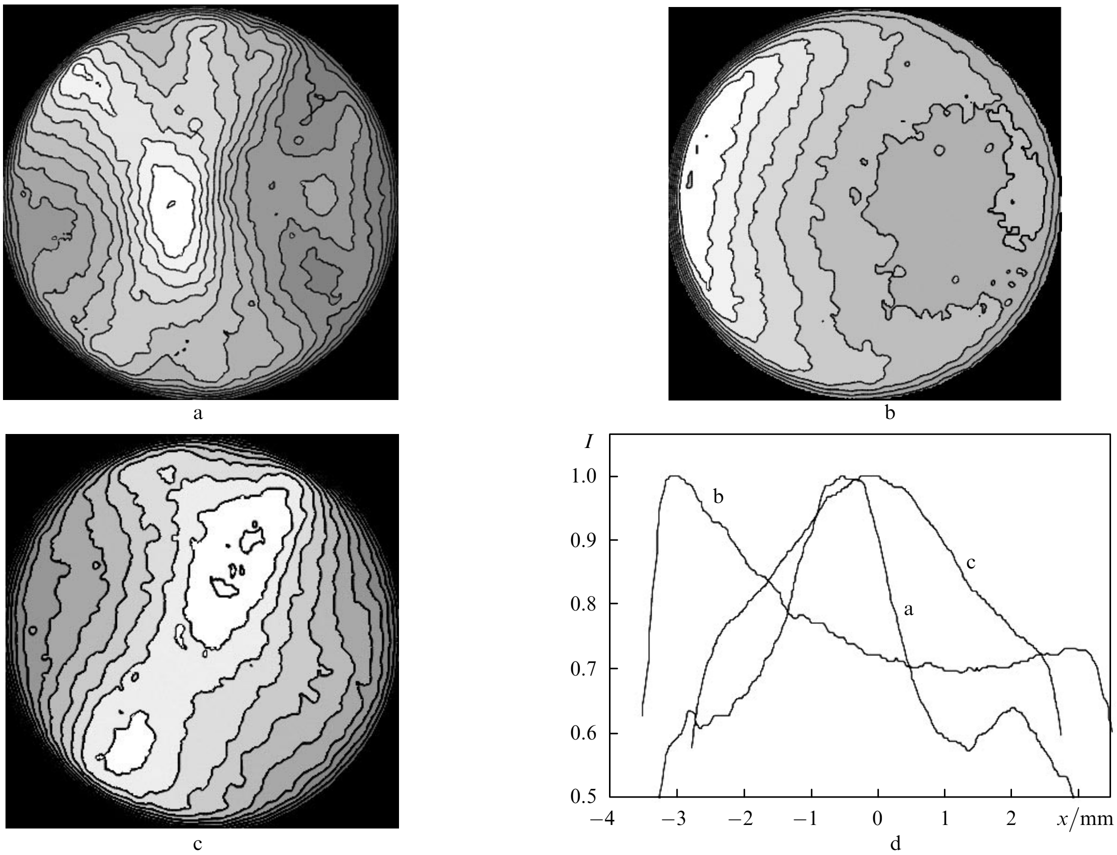

Figure 2. Inverse-population distributions in the GLS-23P glass AE of a laser having monoblock pump cavities with mirror (a, c) and diffusion (b) reflectors [AE diameters are 7 mm (a, b) and 5 mm (c), the pump voltage is 1 kV ($C = 100$ μF), the flashlamp is located to the left of the corresponding distributions] and these distributions normalised to their maximum value in the flashlamp–AE plane (d).

an aperture of diameter 4.2 mm was inserted into the resonator, the LG mode with $N \approx 7$ was emitted (Fig. 3b).

Note that in both cases the order of generated modes changes within a small range from pulse to pulse, and regions with poorly discernible structure of the lobes of LG modes are always observed in the recorded distributions. The first circumstance is probably explained by the insufficient stability of the pump level, and the second – by the experimental conditions because the laser operates in this case in the free-running regime, and distributions presented in Figs 3a, b can be the superposition of distributions in different laser radiation spikes having different types (sin or cos) and different order of the LG modes.

It is not inconceivable that the structure of the LG mode lobes can be distorted due to the specific nature of excitation of LG modes in a laser with the gain distribution having a minimum on the resonator axis. This is confirmed by the numerical calculations of the establishment of types of oscillations in such a laser presented in Figs 3c, d. We used in calculations the parameters of a plane–spherical laser resonator presented above ($L = 50$ cm, $R = 300$ cm). In the case of Fig. 3c, where the distortion of the mode structure is most noticeable, a 6-mm aperture was mounted on the laser AE [$G(r_{\max})/G(0) = 1.1$]. The aperture diameter in Fig. 3d was 4.5 mm [$G(r_{\max})/G(0) = 1.06$].

The HG mode distributions presented in Fig. 4 were obtained by using a mirror reflector and an AE of diameter 5 mm. To excite the HG modes with $N > 0$, one or two thin (80-μm thick) wires were inserted into the resonator, which fixed the position of the zero values of the field of the

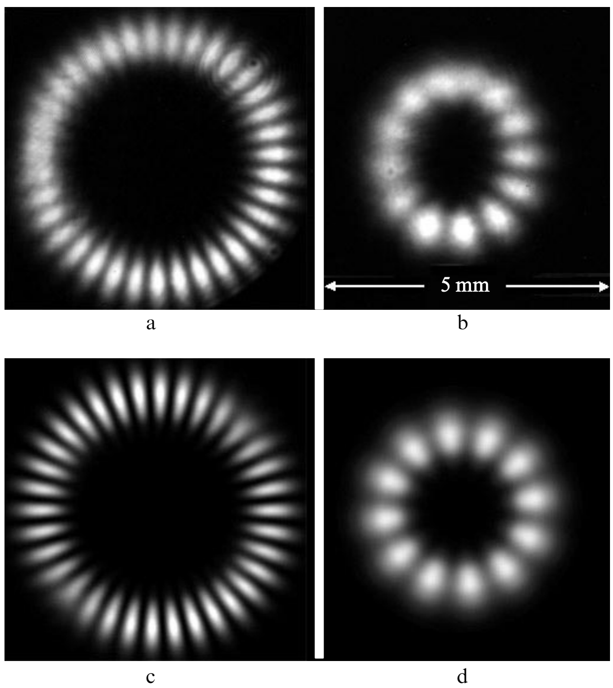

Figure 3. Laguerre–Gaussian modes excited in the Nd^{3+} : laser with a plane–pherical resonator (free-running regime) and the inversion distribution presented in Fig. 2b for resonators with 6-mm and 4.2-mm apertures (a, b), and the Fox–Li calculations for the empty resonator with aperture diameters close to experimental values (c, d). The scale is shown for all the figures.

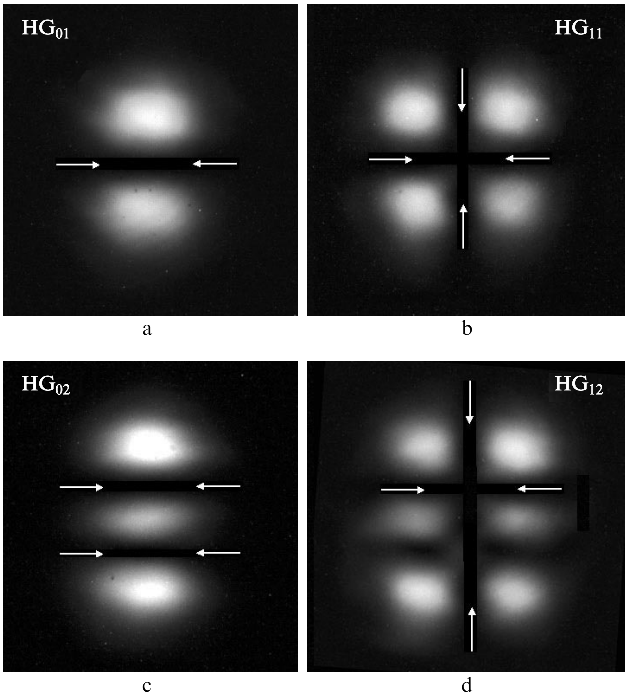

Figure 4. Experimental intensity distributions for HG modes. The arrows indicate the position and orientation of masks (wires of diameter 80 μm) in the laser resonator.

corresponding modes. The position of wires were chosen by the minimum of the lasing threshold and the correspondence of the beam distribution to the specified type of oscillations.

The quality of the HG mode beams was verified by transforming them to the LG modes by using an astigmatic $\pi/2$ converter [15], which was placed at a distance of ~ 75 cm from the output mirror of the laser. Because the beams with the front curvature $\rho = 0$ are eigenbeams for the $\pi/2$ converter with the scheme described in [15], an additional lens with the focal distance 250 cm compensating the spherical component of the wave front was placed in front of the converter. The converter was tuned to the Rayleigh length of the beam being transformed by changing the mutual orientation of its cylindrical lenses (see details in [16]).

The result of the transformation of HG modes, shown in Fig. 4, to the corresponding LG modes is presented in Fig. 5. The distribution curves (along the x axis) for some HG and LG modes are compared with their theoretical values in Fig. 6. We can conclude as a whole that the generation of HG modes of the order up to $N = 3$ in a passively Q-switched solid-state laser by fixing the zero values of the field gives the satisfactory result. If such a fixation is performed not for all zero values (Fig. 4d), this immediately affects the result of transformation to the LG mode (Fig. 5d). In this case, as follows from numerical calculations, various amplitude distortions of the HG modes (for example, the violation of the relation between individual maxima) weakly affect the result of conversion to the LG modes. However, if a different-order mode (or of the same order, but with different transverse indices m and n) of intensity of a few and even tenth factions of percent is added to some HG mode, this considerably distorts the phase distribution of the transformed beam and gives the worse result.

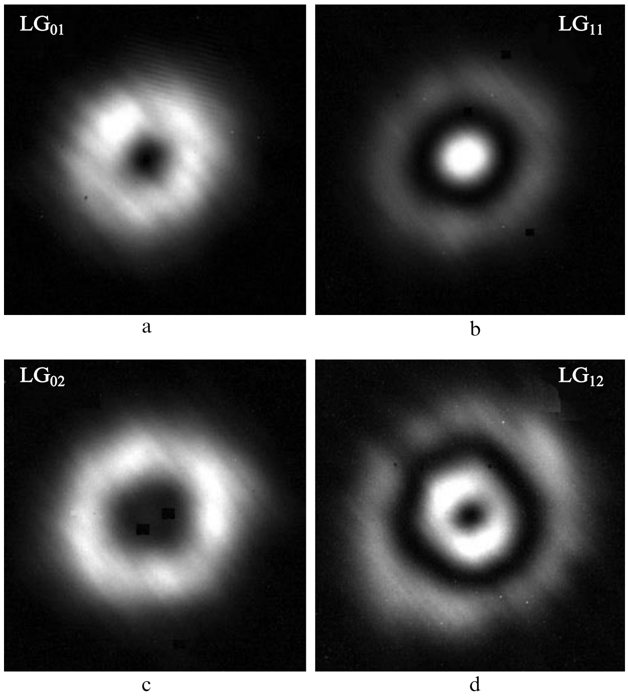

Figure 5. Conversion of the HG modes (Fig. 4) to the LG modes.

Figure 7 demonstrates the distributions of the u_{20}^{HG} mode distorted in different ways and the result of the conversion of these beams to the LG modes. In one case, the intensity of the right maximum of the u_{20}^{HG} mode is weakened by 20 % compared to that of the left maximum (Fig. 7a), while in another (Fig. 7b) the coherent sum of the u_{20}^{HG} mode of the unit energy and the u_{02}^{HG} mode with energy equal to 0.01 of the u_{20}^{HG} mode energy is taken. Figure 7c and d show the result of the transformation of distorted beams. In the first case (Fig. 7c), the distortions of the LG mode is weakly noticeable, although the ratio of the LG mode intensity maximum to its minimum is 1.28, while in the second case the distortions are observed in the form of four maxima and minima with the intensity ratio ~ 1.5 (Fig. 7d).

2.3 Discussion and conclusions

It is known (see, for example, [17]) that the presence of phase and amplitude inhomogeneities in a laser resonator favours the appearance of coupling between the types of oscillation excited in the resonator. An example of amplitude inhomogeneities is the inhomogeneous IP distribution, which causes inhomogeneous thermal distortions in the active medium of a laser, especially in a neodymium glass having the relatively low heat conduction. Recall that the absorption bands of Nd^{3+}, which are not involved in the population of the upper laser level, also make a contribution to heating. Under these conditions, such a coupling is most strong (resonance) in degenerate resonators, for which

$$\frac{2\pi}{\arccos(1 - 2L/R)} = \frac{r}{s}, \tag{6}$$

where r and s are integers.

In this paper, we used a nondegenerate resonator ($L =$ 50 cm, $R = 300$ cm) and used a pump system providing the most homogeneous IP distribution. However, to obtain the

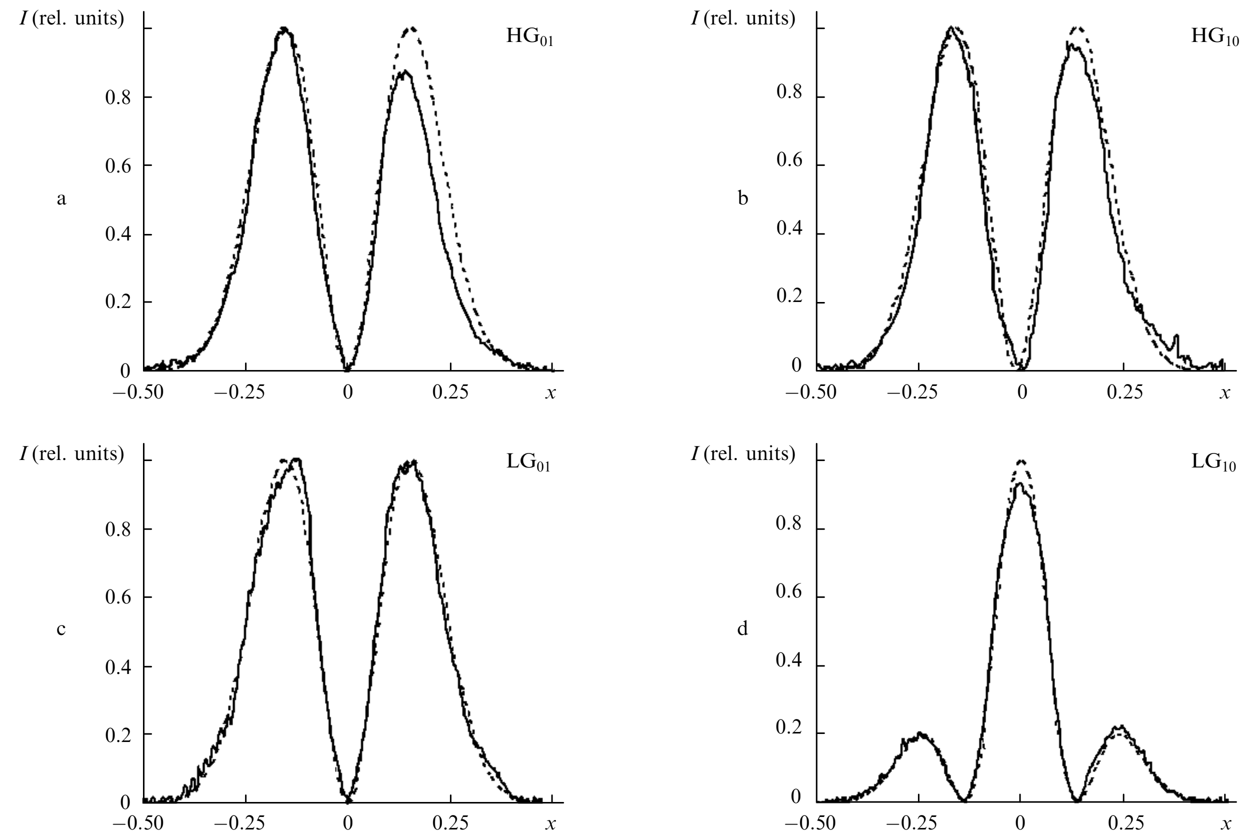

Figure 6. Comparison of the intensity distributions (along the x axis) of some HG (Figs 4a, b) and LG (Figs 5a, b) modes with their theoretical values (dashed curves).

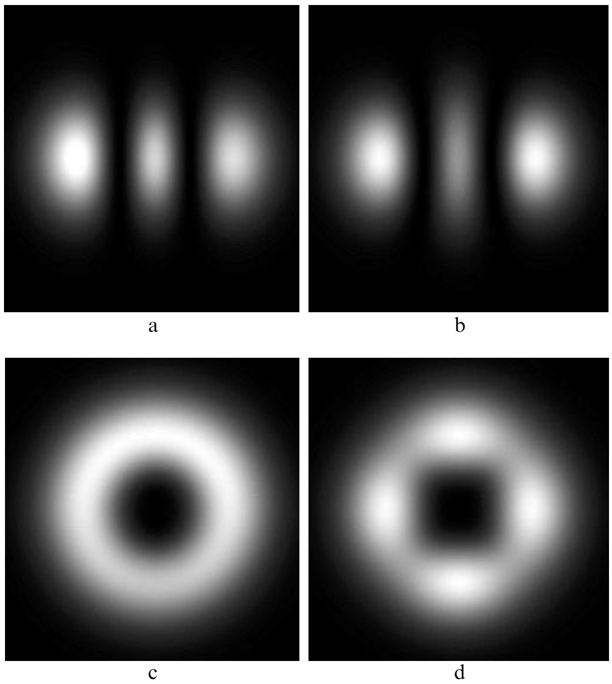

Figure 7. Calculation of the influence of the distortions of the u_{20}^{HG} mode on conversion to the u_{02}^{LG} mode with the help of an astigmatic $\pi/2$ converter (see details in the text).

uniform distribution of inversion (and the gain) with pump cavitiess used in our study, the neodymium concentration in a GLS-23 glass proved to be far from optimal: it was somewhat high for the diffusion reflector and insufficient for mirror reflectors. Nevertheless, we have managed to obtain quite stable and controllable generation of the HG modes up to the third order inclusive in a flashlamp-pumped neodymium phosphate glass laser and converted these modes to the corresponding LG modes. We have also demonstrated that, by using a laser with the IP minimum on the axis of a plane–spherical resonator and varying its Fresnel number, the LG modes [with the field amplitude dependence $\sim {\sin \atop \cos}(l\varphi)$] of different orders can be efficiently excited.

Acknowledgements. The authors thank V.Kh. Bagdasarov, S.V. Garnov, and N.N. Denisov for their great help in the performance of experiments. This work was supported by the Russian Foundation for Basic Research (Grant No. 05-02-16818) and a Grant No. NSh-8283.2006.2 of the President of the Russian Federation for Support of the Leading Scientific Schools.

References

1. ISO 11146 *'Lasers and laser-related equipment: Test methods for laser beam widths, divergence angles and beam propagation ratios»;* ISO 11554 *«Lasers and laser-related equipment: Test methods for laser beam power, energy and temporal characteristics'.*
2. Morin M. *Opt. Quantum Electron.*, **29**, 819 (1997).
3. Beijersbergen M.W., Allen L., van der Veen H.E.L.O., Woerdman J.P. *Opt. Commun.*, **96**, 123 (1993).
4. Malyutin A.A. *Kvantovaya Elektron.*, **33**, 235 (2003) [*Quantum Electron.*, **33**, 235 (2003)].

5. Malyutin A.A. *Kvantovaya Elektron*., **34**, 165 (2004) [*Quantum Electron*., **34**, 165 (2004)].
6. Arlt J., Hitomi T., Dholakia K. *Appl. Phys. B*, **71**, 549 (2000).
7. Molloy J.E., Dholakia K., Padgett M.J. *J. Modern Opt*., **50**, 1501 (2003).
8. Prentice P.A., MacDonald M.P., Frank T.G., Cuschieri A., Spalding G.C., Sibbett W., Campbell P.A., Dholakia K. *Opt. Express*, **12**, 593 (2004).
9. *Proc. Symp. 'Progress In Electromagnetics Research'* (Cambridge, USA, 2006).
10. Malyutin A.A. *Kvantovaya Elektron*., **37**, 299 (2007) [*Quantum Electron*., **37**, 299 (2007)].
11. Egorov A.L., Korobkin V.V., Serov R.V. *Kvantovaya Elektron*., **2**, 513 (1975) [*Sov. J. Quantum Electron*., **5**, 291 (1975)].
12. www.elphel.com
13. Siegman A.E. *Lasers* (Mill Valley, Cal.: Univ. Science Books, 1986) Chpt. 20.
14. Walsh D.M., Knight L.V. *Appl. Opt*., **25**, 2947 (1986).
15. Malyutin A.A. *Kvantovaya Elektron*., **33**, 1015 (2003) [*Quantum Electron*., **33**, 1015 (2003)].
16. Malyutin A.A. *Kvantovaya Elektron*., **36**, 79 (2006) [*Quantum Electron*., **36**, 79 (2006)].
17. Paschotta R. *Opt. Express*, **14**, 6069 (2006).